Identification of an ABCB/P-glycoprotein-specific Inhibitor of Auxin Transport by Chemical Genomics*[S]

Jun-Young Kim[‡1]**, Sina Henrichs**[§1]**, Aurélien Bailly**[§]**, Vincent Vincenzetti**[§]**, Valpuri Sovero**[§]**, Stefano Mancuso**[¶]**, Stephan Pollmann**[∥]**, Daehwang Kim**[**]**, Markus Geisler**[§2]**, and Hong-Gil Nam**[‡3]

From the ‡*Laboratory of Plant Systems Bio-Dynamics, Pohang University of Science and Technology, 790-784 Pohang, Korea, the* §*Institute of Plant Biology, University of Zurich and Zurich-Basel Plant Science Center, Zolliker Strasse 107, CH-8008 Zurich, Switzerland, the* ¶*Department of Horticulture, University of Firenze, I-50019 Sesto Fiorentino, Italy, the* ∥*Lehrstuhl für Pflanzenphysiologie, Ruhr-Universität Bochum, D-44801 Bochum, Germany, and the* **Biomaterials Research Center, Korea Research Institute of Chemical Technology, 305-600 Dae-jon, Korea*

Plant development and physiology are widely determined by the polar transport of the signaling molecule auxin. This process is controlled on the cellular efflux level catalyzed by members of the PIN (pin-formed) and ABCB (ATP-binding cassette protein subfamily B)/P-glycoprotein family that can function independently and coordinately. In this study, we have identified by means of chemical genomics a novel auxin transport inhibitor (ATI), BUM (2-[4-(diethylamino)-2-hydroxybenzoyl]benzoic acid), that efficiently blocks auxin-regulated plant physiology and development. In many respects, BUM resembles the functionality of the diagnostic ATI, 1-*N*-naphtylphtalamic acid (NPA), but it has an IC_{50} value that is roughly a factor 30 lower. Physiological analysis and binding assays identified ABCBs, primarily ABCB1, as key targets of BUM and NPA, whereas PIN proteins are apparently not directly affected. BUM is complementary to NPA by having distinct ABCB target spectra and impacts on basipetal polar auxin transport in the shoot and root. In comparison with the recently identified ATI, gravacin, it lacks interference with ABCB membrane trafficking. Individual modes or targets of action compared with NPA are reflected by apically shifted root influx maxima that might be the result of altered BUM binding preferences or affinities to the ABCB nucleotide binding folds. This qualifies BUM as a valuable tool for auxin research, allowing differentiation between ABCB- and PIN-mediated efflux systems. Besides its obvious application as a powerful weed herbicide, BUM is a *bona fide* human ABCB inhibitor with the potential to restrict multidrug resistance during chemotherapy.

In plants, the auxin indolyl-3-acetic acid (IAA)[4] serves as a hormone-like signaling molecule that is a key factor in plant development and physiology (1–4). Many of its functionalities are controlled by a unique, plant-specific process, the cell-to-cell or polar auxin transport (PAT) (3). However, cellular efflux is the rate-limiting step of PAT, and in agreement with the chemiosmotic hypothesis, putative exporters of the PIN (pin-formed) and B subfamily of ABC transporter, ABCB/PGP/MDR (P-glycoprotein, multidrug resistance), families have been identified (5–7).

Most PIN efflux carriers show predominantly polar locations in PAT tissues and developmental, organogenetic loss-of-function phenotypes and are thought to be the determinants of a "reflux loop" in the root apex (3, 8). ABCB isoforms have been identified as primary active (ATP-dependent) auxin pumps showing auxin-related, developmental (but not organogenetic) loss-of-function phenotypes (5, 9, 10). Despite their mostly apolar locations, they have been demonstrated to contribute to PAT and long range auxin transport (5, 11, 12). Moreover, ABCB1/PGP1 and ABCB19/PGP19/MDR1 coordinately function in basipetal reflux of auxin maxima out of the root and shoot tip (9). The immunophilin-like FKBP42, TWD1 (twisted DWARF1) protein, was characterized as a central regulator of ABCB-mediated auxin transport by means of protein-protein interaction (11, 12). Positive regulation of ABCB1- and ABCB19-mediated auxin transport accounts for overlapping phenotypes between *twd1* and *abcb1 abcb19* (11, 12).

ABCB- and PIN-mediated auxin efflux can function independently and play identical cellular but separate developmental roles (10). However, ABCBs and PINs are also able to interactively and coordinately transport auxin (9). The current picture that emerges is that in interacting cells, multilaterally expressed ABCBs minimize apoplastic reflux, whereas polar ABCB-PIN interactions provide specific vectorial auxin stream (10). However, the individual roles of ABCB- and PIN-mediated auxin flows are far from being understood.

The investigation of PAT streams was facilitated by using synthetic compounds that act as auxin transport inhibitors (ATIs), with the non-competitive IAA efflux inhibitor 1-*N*-naphtylphtalamic acid (NPA) being the most prominent. Until today, the identity, number, and affinity of putative NPA-bind-

An ABCB/P-glycoprotein-specific Inhibitor of Auxin Transport

ing proteins (NBPs) is still controversial (13–17). However, the current consensus is that the auxin efflux complex consists of at least two proteins: a membrane-integral transporter and an NBP-regulatory subunit (13–15, 18). Several lines of evidence suggest that PIN proteins do not themselves act as NBPs (19), although NPA application results in a pin-formed inflorescence, mimicking *PIN1* loss of function (20). Therefore, it was suggested that NPA blocks PAT by interfering with the cycling of auxin transporters, like PIN1 (21). However, NPA itself does not directly affect PIN cycling, and concentrations necessary to perturb PIN cycling were much higher than was needed for efficiently blocking PAT (16, 21). Independently, ABCB1 and ABCB19 have been identified as targets of NPA (5, 22, 23) and high affinity NBPs (23–25). Surprisingly, NPA was additionally shown to bind to TWD1, and NPA binding disrupted TWD1-ABCB1 interaction (11). *In planta*, this leads to disruption of ABCB1 activity, suggesting that TWD1 and ABCB1 represent high and low affinity components of the NPA-sensitive efflux complex (11).

In the last few years, chemical genomic screens have allowed for the identification of several synthetic compounds and, in some cases, respective molecular targets that interfere with auxin signaling (26, 27), membrane trafficking (28–30), and auxin transport (23, 31). 3-(5-[3,4-dichlorophenyl]-2-furyl)-acrylic acid (gravacin) was recently identified as a strong inhibitor of root and shoot gravitropism, auxin responsiveness, and protein trafficking to the tonoplast in *Arabidopsis* (30). In a follow-up screen, inhibition of gravitropism and protein trafficking was shown to employ independent mechanics (23). Mutations in *ABCB19* confer resistance to the effect of gravacin on hypocotyl gravitropism and result in reduced binding of gravacin to microsomal fractions, implicating ABCB19 as the major target of gravacin (23). Consequently, gravacin was found to be a strong inhibitor of ABCB19-mediated auxin transport in *Arabidopsis* and HeLa cells.

In this study, we screened chemical libraries of small organic compounds for plant physiological and developmental regulators and identified a novel, highly potent ATI by means of chemical genomics. A direct comparison of compound 10824 (BUM) and NPA effects on auxin-controlled plant physiology, auxin transport, and drug binding reveals that BUM shares many features with NPA, like induction of pin-formed inflorescences and ABCB binding and blocking of transport. Unlike NPA and gravacin, BUM lacks growth activation at lower concentrations and does not interfere with membrane trafficking, respectively. BUM might therefore act as a powerful tool in dissecting ABCB- and PIN-mediated auxin streams in plant physiology.

EXPERIMENTAL PROCEDURES

Chemical Library Screens—*Arabidopsis thaliana* ecotype Columbia (Col) seeds were surface-sterilized, stratified at 4 °C for 3 days, and grown horizontally in 24-well plates (3 seeds/well; 0.5× B5 medium, 2% sucrose, 0.8% agar) at 22 °C under continuous light. Seven days after germination (dag), 2 μM organic compounds of a chemical library (containing 6,500 small organic chemicals at 50 μM in DMSO) from the Korea Chemical Bank was added manually. Plant phenotypes in respect to plant morphology, growth rate, leaf color, flowering time, and senescence were monitored every 2 days by visual

examination in comparison with the solvent (DMSO) control on each plate up to 14 dag.

In a secondary screen, plants were treated with various concentrations (up to 10 μM) of compounds from the Korea Chemical Bank that were structurally related to compound 10824 and thus contained the 2-(formyl)-benzoic acid core (Fig. 1*B* and supplemental Fig. S1). Phenotypes were screened for induction of pin-formed inflorescences (see Fig. 1*C*).

Plant Material and Quantification of Growth—For long term experiments, *abcb1/pgp1–1* (At2g36910), *abcb19/pgp19–1/mdr1-1* (At3g28860) (all ecotype Wassilewskija), and *pin2/eir1-4* (At5g57090, ecotype Columbia) were grown on 0.5× B5 medium, 2% sucrose, 0.8% phytagar under continuous light for 18 dag in sterilized plastic boxes (SPL, Korea). For all other experiments, seedlings were grown if not indicated otherwise for 5 dag on vertical plates containing 0.5× Murashigge and Skoog medium, 1% sucrose, 1% phytagar in the dark or at 16 h of light/day. For growth quantification, seedlings were transferred on drug-containing plates (0 –50 μM). After 5, 7, 9, and 11 dag, seedlings were aligned on 1% phytoagar medium, images were scanned, and root and hypocotyl lengths and lateral root numbers (7, 9, and 11 dag) were measured using Scion Image software (Scion Corp., Frederick, MD). For determination of IC_{50} values, root lengths of 7-dag seedlings grown on 0–80 μM NPA and 0–20 μM BUM were quantified, and IC_{50} values were calculated using sigmoidal dose-response fits. All experiments were performed at a minimum as triplicates with 20–30 seedlings per experiment.

In Planta Analysis of Auxin Responses and Transport—Homozygous F4 generations of *A. thaliana* wild-type, *pin2/eir1-4* (32), *abcb1/pgp1–1*, and *abcb19/pgp19-1/mdr1-1* (25) mutants expressing the maximal auxin-inducible reporter Pro$_{DR5}$:GFP (41) were grown vertically for 5 dag and analyzed by confocal laser-scanning microscopy (Leica; DMIRE2). In some cases, seedlings were transferred for an additional 12 h onto new plates containing 0.5 μM BUM, 5 μM NPA, or the solvent DMSO. For histological signal localization, differential interference contrast and GFP images were merged electronically using Photoshop 10.0.1 (Adobe Systems).

For measurements of basipetal root and hypocotyl (shoot) transport, seedlings were grown for 9 or 7 dag on vertical plates containing 0.5× Murashigge and Skoog medium, 1% sucrose, 1% phytagar at 16 h of light/day at 100 microeinsteins (root) or 10 microeinsteins (hypocotyl), respectively. Measurements were performed as described in Ref. 33, using radiolabeled IAA that was applied by placing solified agar droplets next to the seedlings root tips or at the apical (cut) end of the hypocotyls. In some cases, solified IAA droplets contained 1 μM BUM or 10 μM NPA. Data are means of three independent experiments with each four replica of 10 seedlings each.

A platinum microelectrode was used to monitor IAA fluxes in *Arabidopsis* roots as described previously (11, 12, 34, 35). For measurements, plants were grown in hydroponic cultures and used at 5 days after germination. Differential current from an IAA-selective microelectrode was recorded in the absence and presence of 5 μM NPA, BUM, or gravacin (23).

Endogenous free IAA was quantified from shoot and root segments of MeOH-extracted seedlings by using gas chroma-

tography-mass spectrometry, as described by Bouchard *et al.* (12). Seedlings were analyzed after 24-h treatments with 5 μM NPA or 0.5 μM BUM. Data are means of four independent lots of 40–50 seedlings each.

Yeast Auxin Loading Assays—PIN1,2- and ABCB1,19-mediated IAA transport was measured by assaying IAA loading into *Schizosaccharomyces pombe* mutant strains *ael1* and *mam1 pdr1*, respectively, as described (36), with the following modifications. Retained radioactivity was quantified by vacuum filtration after 0 and 10 min of incubation at 30 °C, and inhibitors at 10 μM were added for 30 min prior to loading and during loading. Relative ABCB1,19- and PIN1,2-mediated IAA and benzoic acid (BA) loading is calculated from retained radioactivity as follows: (radioactivity in the yeast at $t = 10$ min) − (radioactivity in the yeast at $t = 0$)) × (100%)/(radioactivity in the yeast at $t = 0$ min). Presented are mean values from four independent experiments (independent transformants) with four replicates each.

NPA Binding Studies—NPA binding assays using *Arabidopsis* or yeast microsomes were performed as described elsewhere (11). In short, four replicates of 10 μg each of protein were incubated with 10 nM [³H]NPA (80 Ci/mmol) and 10 nM [¹⁴C]BA (55 mCi/mmol) in the presence and absence of 10 μM NPA. For competition experiments, 10 μM BUM was added. Reported values are the means of specific binding ([³H]NPA bound in the absence of cold NPA (total) minus [³H]NPA bound in the presence of cold NPA (nonspecific)) from four independent experiments (independent transformants) with four replicates each.

Point mutations E502K and F792K in ABCB1 (pNEV-PGP1 (5)) were introduced using the QuikChange XL site-directed mutagenesis kit (Stratagene, La Jolla, CA), resulting in pNEV-ABCB1^E502K and pNEV-ABCB1^F792K (see Fig. 6B).

BRET Analysis—Microsomes from yeast JK93da expressing PGP1-YFP and TWD1-rLuc (11) were prepared in the presence or absence of 5 μM NPA, BUM, or gravacin or adequate amounts of solvents. BRET signals were recorded in the presence of 5 μM coelenterazine (Biotium Inc.), and BRET ratios were calculated as described (11). The results are the average values from four independent experiments with four replica each of 10 readings collected every minute.

Data Analysis—Data were analyzed using Prism 4.0b (GraphPad Software, San Diego, CA). *A. thaliana* ABCB1 structure modeling was performed using PyMOL version 0.99 (DeLano Scientific LLC, San Carlos, CA) and maximum entropy-based ligand binding was computed using MEDock (available on the World Wide Web). Drug docking was confirmed by using ZDOCK (available on the World Wide Web). Drug three-dimensional structures were energy-minimized using PRODRG2 (available on the World Wide Web), and solely polar hydrogens are displayed (usual atom *color code*).

RESULTS

A Chemical Library Screen for Growth and Developmental Regulators—To identify growth and developmental regulators, we screened *A. thaliana* (ecotype Columbia; Col Wt) seedlings with a chemical library (Korean Chemical Bank, KRICT, Korea) composed of 6,500 small organic compounds. Seeds were germinated in 24-well plates, and at 7 dag, a 2 μM concentration of
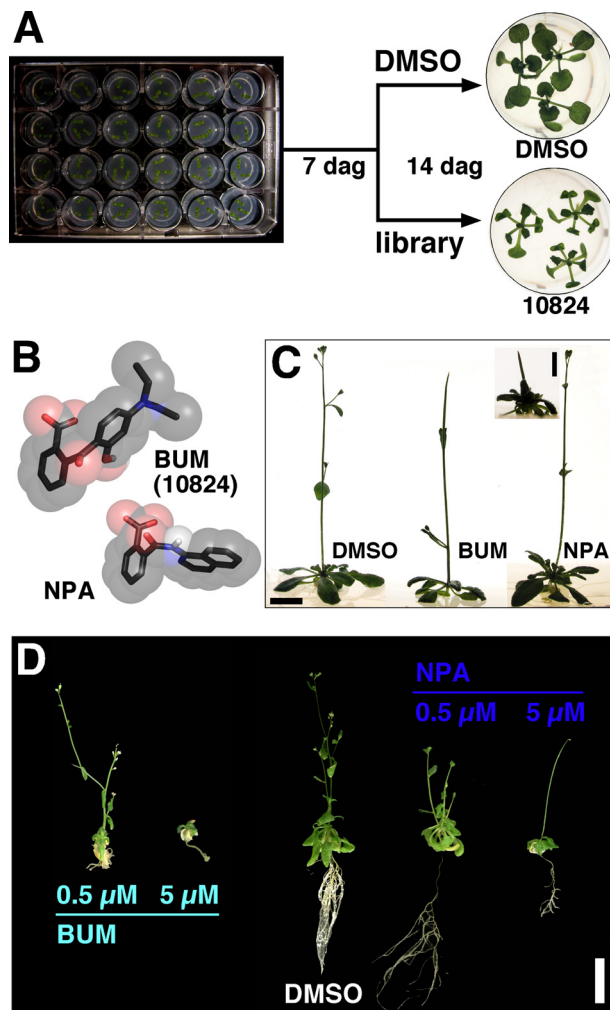

FIGURE 1. **A chemical genomic screen identified a novel auxin transport inhibitor-like compound inducing pin-formed inflorescences.** *A*, a microtiter-based screening strategy using a chemical library from the Korean Chemical Bank identified compound 10824 (BUM) as a strong modifier of plant development. *B*, three-dimensional structures of BUM in comparison with established auxin efflux inhibitor, NPA. *C*, BUM-induced pin-formed inflorescences. Note that BUM concentrations necessary for pin-formed inflorescence induction are roughly 20-fold lower compared with NPA (10 μM NPA; *inset*). *D*, BUM strongly reduces primary root growth, which is not found with NPA. *Scale bars*, 2 cm.

a different library compound was added to each well. Plant phenotypes with respect to plant morphology, growth rate, leaf color, flowering time, and senescence were monitored every 2 days by visual examination in comparison with solvent (DMSO) controls. Among the various chemical compounds that led to altered plant morphology, compound number 10824 (2-[4-(diethylamino)-2-hydroxybenzoyl]benzoic acid) produced a drastic phenotype, including dark green, epinastic leaves (Fig. 1*A*), suppression of primary and secondary roots (Fig. 1*D*), and abnormal, pin-formed inflorescences (Fig. 1*C*). We narrowed our focus to this compound 10824, subsequently named BUM,⁵ verifying consistently growth inhibition under a variety of assay conditions in follow-up screenings.

---

⁵ Named after the famous Korean football player, Cha Kun-Bum. BUM is available for academic institutions upon request from M. G.

An ABCB/P-glycoprotein-specific Inhibitor of Auxin Transport

The fact that BUM/10824 produced pin-formed inflorescences in analogy to the well established ATI, NPA (15, 16, 37), and that both contain a 2-(formyl)-benzoic acid core (Fig. 1*B*), prompted us to compare growth defects between BUM and NPA over a wide concentration range. BUM induces pin-shaped inflorescences and reduces primary root growth at 0.5 μM, which is roughly 20 times lower than what is needed for NPA (Fig. 1, *C* and *D*).

In a secondary screen, we tested compounds that contained a 2-(formyl)-benzoic acid core taken from the Korea Chemical Bank and Chembridge chemical libraries. None of the six tested compounds A–F was able to induce pin-shaped inflorescences over a wide concentration range up to 10 μM (supplemental Fig. S1), suggesting that not the 2-(formyl)-benzoic acid core alone but side chains determine functionality.

BUM Affects Auxin-controlled Plant Growth—These findings suggested that BUM influences plant growth and development in analogy to the ATI, NPA, but has a stronger effect. Therefore, we quantified root and hypocotyl lengths, known to be inversely controlled by auxin, in the presence of BUM and NPA in more detail. BUM drastically reduced primary root growth of light-grown wild type seedlings (Fig. 2, *A* and *B*) with an apparent IC_{50} of 0.4 μM (supplemental Fig. S5), which is roughly a factor of 30 less than what is needed with NPA (IC_{50} = 12.8 μM). A similar effect was found also for hypocotyl elongation of light-grown seedlings. NPA shows, in agreement with previous reports on roots (38), a stimulating and inhibitory result upon hypocotyl elongation under light at nanomolar and micromolar concentrations, respectively. Such a biphasic behavior was not found for BUM in the concentration range used (0–20 μM), suggesting, despite widely overlapping effects, a different mode of action or targets (Fig. 2).

A shoot-derived auxin pulse known to be efficiently inhibited by NPA (39–41) tightly controls lateral root emergence (42). Not unexpectedly, 0.1 μM BUM drastically blocked lateral root formation in both of the tested *Arabidopsis* ecotypes, Col and Ws, by roughly 50%; enhanced sensitivities compared with 0.5 μM NPA (roughly 25% inhibition) were in line with what was found for primary root growth.

Interestingly, root and hypocotyl growth inhibition by BUM and NPA was light-dependent and less pronounced in dark-grown, etiolated seedlings (supplemental Fig. S4). Moreover, shoot hook formation and opening of etiolated seedlings was inhibited by 5 μM BUM but not by NPA (Fig. 2*A*), which requires higher concentrations, as was shown before (43–45). This is in agreement with the concept that auxin has a more important role in elongation and bending responses in light-grown than in dark-grown seedlings (44, 45).

Next we tested root gravitropism, another hallmark of auxin-controlled plant physiology (46, 47). BUM disrupted root bending in wild type seedlings drastically (supplemental Fig. S2). Interestingly, the ecotype Col revealed higher sensitivities (77% inhibition) compared with the ecotype Ws (58% inhibition) not found for NPA (11, 38). Similarly to lateral root formation, 0.1 μM BUM (supplemental Fig. S2) was more efficient than 5 μM NPA assayed in both ecotypes in parallel (not shown) (11, 38). Recently, single loss-of-function roots, *pin2*, *abcb1*, or *abcb19*, were shown to be NPA-sensitive using gravitropism assays (11,
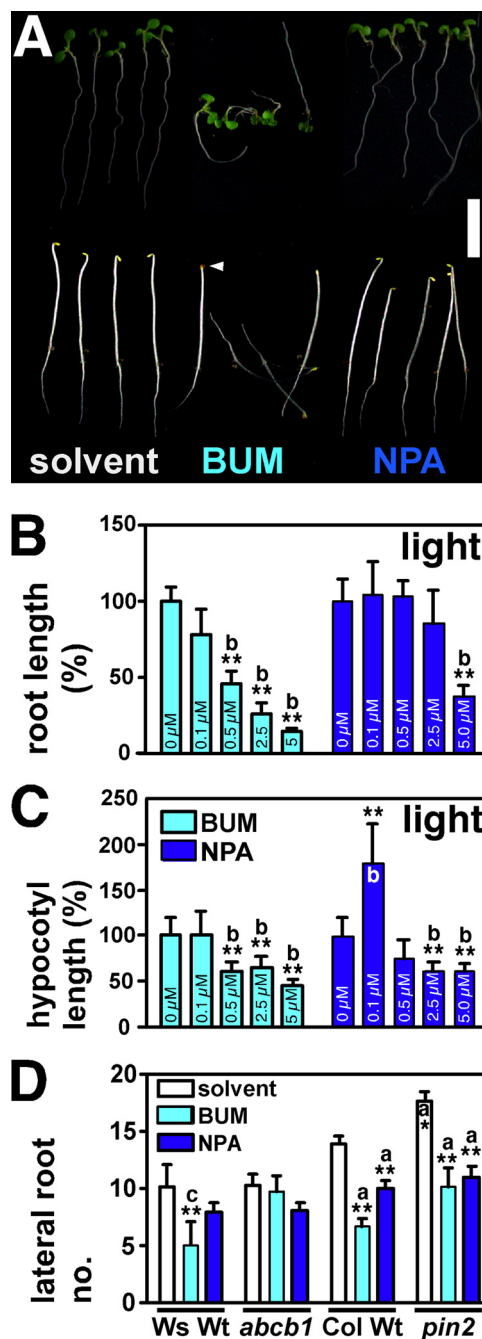

FIGURE 2. **BUM reduces root and hypocotyl growth in the light.** *A*, phenotype of BUM- and NPA-treated (each 0.5 μM) light- (*top*) and dark-grown (*bottom*) seedlings 5 dag (days after germination). Note that seedlings grown in the presence of BUM are hookless (*white arrow*). *Scale bar*, 1 cm. *B* and *C*, dose dependence of BUM and NPA treatments on primary root (*C*) and hypocotyl (*D*) lengths; absolute root and hypocotyl lengths were 29.5 ± 4.4 and 2.7 ± 0.5 mm, respectively. *D*, reduction of lateral root numbers caused by BUM (0.1 μM) and NPA (0.5 μM) treatments 11 dag. Note that *abcb1* in contrast to wild-type and *pin2* is less sensitive to BUM. Data are mean ± S.D. (*error bars*) (n = 3 with each 20–30 seedlings). Significant differences from wild type or between inhibitor and solvent treatments (0 μM) are indicated by *one* or *two asterisks*, respectively, and were calculated using Dunnett's multiple comparison test (*A* and *B*) or analysis of variance (*C*) (Tukey's test for multiple comparisons) with the following p values: $p < 0.001$ (*a*); $p < 0.01$ (*b*); $p < 0.05$ (*c*).

38). In agreement, DR5-GFP imaging (Fig. 3) revealed no dramatic differences between *pin2* and *abcb1* roots in comparison with corresponding wild types. However, based on gravitropism assays (supplemental Fig. S2) and in contrast to what was
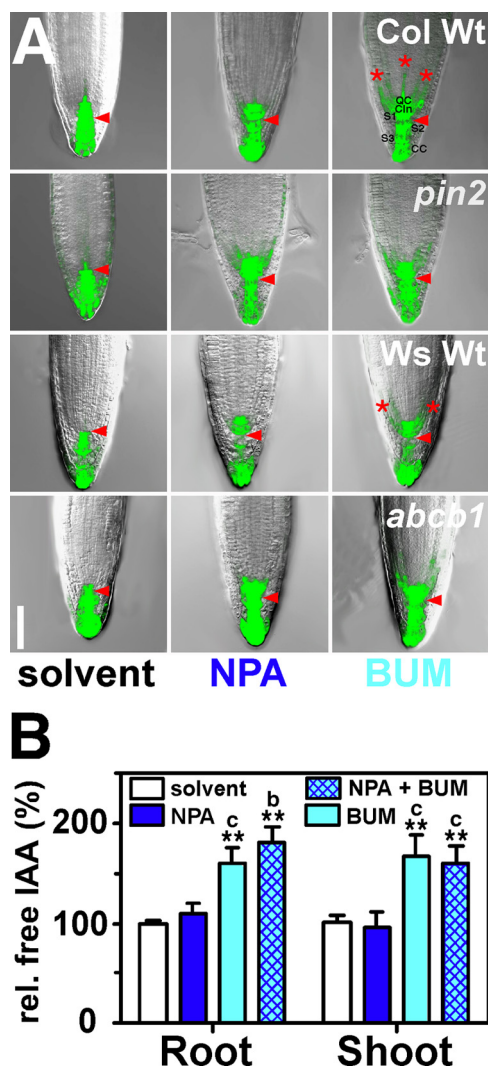
FIGURE 3. **BUM alters auxin responses and levels *in planta*.** *A*, expression of the auxin-responsive reporter DR5-GFP (*green*) upon BUM (0.5 μM) and NPA (5 μM) treatments (24 h) in root tips. BUM and NPA enhance DR5-GFP signals in the quiescent center (*QC*), columella initials (*CIn*), and S1 cells but reduce signals in columella S2, S3, and cap cells (*CC*); S2 and S3 borders are marked with *arrowheads*. Note stronger extensions of GFP signals from quiescent center, columella initials, and S1 cells into initials of epidermis, endodermis, and stele upon BUM treatment (*asterisks*) compared with NPA. *Scale bar*, 200 μm. *B*, root and shoot free IAA concentrations of BUM-treated (0.5 μM) and NPA-treated (5 μM) wild type seedling. Data are mean $\pm$ S.D. (*error bars*) (*n* = 4 with each 40–50 seedlings); absolute wild-type values were 42.2 $\pm$ 5.7 and 49.9 $\pm$ 6.1 pg/mg (fresh weight) for roots and shoots, respectively. Significant differences (analysis of variance using the Tukey's test for multiple comparisons: $p < 0.001$ (*a*); $p < 0.01$ (*b*); $p < 0.05$ (*c*)) between inhibitor and solvent treatments are indicated by *two asterisks*.

recently found for NPA (11, 38), *abcb1* roots were significantly less affected by BUM: 35.3% (percentage occurrence of 60, 90, and 120° bending between inhibitor and solvent control (see "Experimental Procedures")) of *abcb1* roots bent efficiently on BUM but only 26.8% of the corresponding wild type. Even higher resistance was found for *pin2* root gravitropism (supplemental Fig. S2). However, similar inhibition by BUM in the wild type suggests that this is mainly due to the strong genetic effect of the *pin2* mutation. Only partial resistance found for *abcb1* toward BUM is probably caused by functional redundancy between ABCB1 and ABCB19 that was recently confirmed by the finding that *abcb1abcb19* and *twd1* roots have

reduced sensitivities toward NPA (11). These results provide evidence that BUM, like NPA, blocks many aspects of plant physiology that are controlled by the polar transport of auxin.

BUM Alters Auxin Accumulation—To test our conclusions derived from growth experiments and to substantiate the physiological relevance of the proposed BUM function *in planta*, we investigated BUM sensitivity of wild type roots in comparison with NPA using two different approaches. First, analysis of the auxin-responsive reporter construct Pro_{DR5}:GFP (48) revealed that in analogy to NPA (11), BUM disrupts basipetal, root-to-shoot auxin reflux and enhanced the DR5-GFP signal in the quiescent center (*QC*), columella initials (*CIn*), and S1 cells but reduced signals in columella S2 and S3 and cap cells (*CC*) (Fig. 3*A*). BUM inhibition, although used at 10-fold lower concentration, was more drastic compared with NPA, resulting in enhanced DR5-GFP signal extending the quiescent center, columella initials, and S1 cells into initials of epidermis, endodermis, and stele upon BUM treatment (*asterisks*) compared with NPA. As shown before, this inhibitory effect was more pronounced in the Col ecotype than in the Ws ecotype (11).

Second, we analyzed free auxin (*IAA*) levels in vertically grown root and shoot portions of 5-dag wild type seedlings treated with BUM and NPA. Although 5 μM NPA had only a minor effect on auxin root/shoot ratios, 0.5 μM BUM significantly enhanced both root and shoot auxin levels (Fig. 3*B*), suggesting a block of basipetal delivery of IAA from the shoot to the root and *vice versa*. Elevated auxin levels are in agreement with and explain reduced root lengths caused by BUM. Effects of NPA and BUM treatments were not additive (Fig. 3*B*), indicating overlapping modes of action and/or targets. In summary, these data support the concept that BUM in analogy to NPA blocks PAT.

BUM Modifies PIN but Not ABCB1 Expression—Inhibition of PAT-driven plant growth and gravitropism can be achieved via two pathways, by blocking the trafficking (21, 22) and by the direct or indirect inhibition of auxin transporters. Accordingly, gravacin was identified in a chemical genomics screen for gravitropic modulators and shown to block trafficking of the vacuolar marker GFP-∂TIP and ABCB19 but also to bind to and inhibit ABCB19 (23). Therefore, we questioned whether BUM would interfere with the abundance and location of the major players in basipetal auxin transport, ABCB1 and ABCB19 on one hand and PIN1 and PIN2 on the other. Although BUM (like NPA) had only mild effects on the expression (ABCB1 was slightly up-regulated in the stele) and no significant effect on the location of ABCB1- and ABCB19-GFP fusion, NPA and, more pronouncedly, BUM enhanced PIN1-GFP and lowered PIN2-GFP signals in the stele and epidermal/cortical cell files, respectively (Fig. 4). Unchanged expression of ABCB proteins and reduced PIN2 abundance upon BUM and NPA addition is supported by semiquantitative reverse transcription-PCR analysis (supplemental Fig. S3) and for NPA as well by gene chip analysis (see the Genevestigator site on the World Wide Web).

Interestingly, NPA and, again more strongly, BUM induced ectopic PIN1-GFP expression in PIN2 locations (epidermis and cortex; see Fig. 4, *inset*), as described previously for the auxin transport modulator quercetin (38, 49). In light of these findings, up- and down-regulation of PIN proteins in their non-
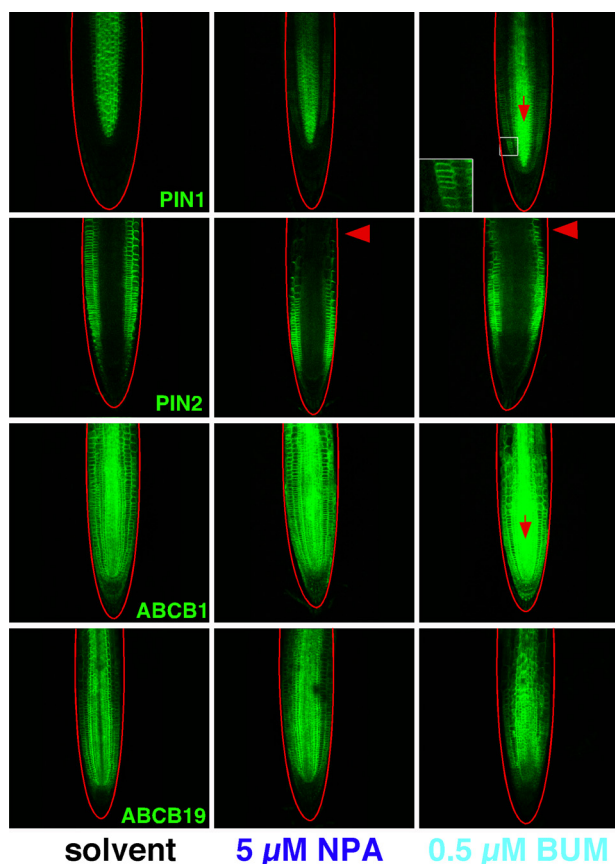
FIGURE 4. **Effect of BUM and NPA on PIN and ABCB abundance and locations.** Localization of PIN1-GFP, PIN2-GFP (8), ABCB1-GFP, and ABCB19-GFP (10) fusion proteins (*green*) in *Arabidopsis* roots 5 dag upon BUM (0.5 μM) and/or NPA (5 μM) treatments (24 h). Note enhanced polar (*arrowheads*) and non-polar PIN1 signals in PIN2 locations upon BUM (*inset*) and NPA treatments and reduced PIN2 expression upon NPA treatment in the elongation zone (*arrowheads*). Root borders are marked in *red*.
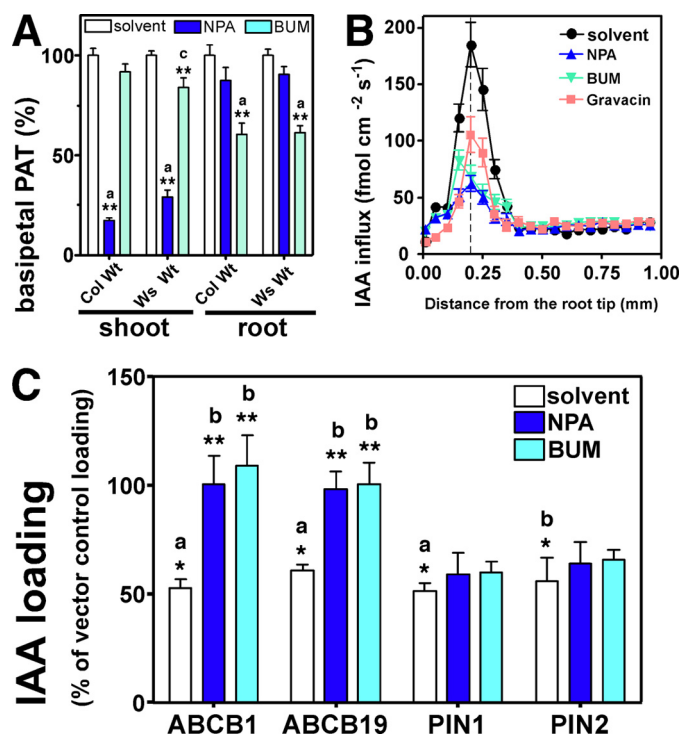

FIGURE 5. **BUM inhibits ABCBs and polar auxin transport in the root.** *A*, BUM and NPA inhibit basipetal IAA transport in roots, whereas NPA (and, to a lesser extent, BUM) blocks basipetal movement in the shoot. Note that concentrations for NPA and BUM were 10 and 1 μM, respectively. Shown are means of three independent experiments $\pm$ S.E. (*error bars*) with each four replicates of 10 seedlings. *B*, IAA influx profile along wild type roots in the presence of inhibitors (5 μM) measured using an IAA-specific microelectrode; positive fluxes represent a net IAA influx. Data are means $\pm$ S.E. ($n = 12$). Note that BUM results in a reduced influx peak at 200 nm from root tip (*red line*) that is shifted apically. *C*, BUM and NPA (each 10 μM) specifically inhibit ABCB1,19-mediated IAA export in the yeast *S. pombe*. ABCB1-, ABCB19-, PIN1-, and PIN2-mediated export was 52.7.2 $\pm$ 4.3, 60.9 $\pm$ 2.8, 51.5 $\pm$ 3.6, and 56.1 $\pm$ 10.6%, respectively, of the corresponding solvent vector control (mean $\pm$ S.E.; $n = 4$). Significant differences (analysis of variance using Tukey's test for multiple comparisons: $p < 0.001$ (*a*); $p < 0.01$ (*b*); $p < 0.05$ (*c*)) from vector controls or between inhibitor and solvent treatments are indicated by *one* or *two asterisks*, respectively.

native environments might be of an indirect nature and triggered by elevated auxin levels in these tissues caused by the blocking of PAT. An inverse impact of IAA on PIN1 and PIN2 expression was reported recently (38, 49, 50). In summary, BUM has, unlike gravacin, only a minor impact on ABCB expression and abundance, but it, like NPA, indirectly interferes with PIN expression probably via altered IAA levels.

BUM Alters Auxin Responses and Levels—Next we aimed to analyze the impact of BUM on PAT *in planta* using two independent approaches. First, we measured polar basipetal root and shoot (hypocotyl) transport of radiolabeled IAA that was applied by placing solified agar droplets next to the seedling root tips or at the apical (cut) end of the hypocotyls using recently described standard protocols (33). In agreement with DR5-GFP auxin reporter analysis, 1 μM BUM inhibited root basipetal (up) PAT in both commonly used *Arabidopsis* wild-type ecotypes, Ws and Col, by roughly 40% (Fig. 5*A*). In contrast, 10 times higher NPA concentrations had only a mild effect, as described in Refs. 42 and 46), where 100 μM NPA was needed for a roughly 30% inhibition. Shoot basipetal (down) PAT IAA transport, known to be (in contrast to root PAT) highly NPA-sensitive (46), was strongly reduced (70–80%) by 10 μM NPA but, surprisingly, less effected by 1 μM BUM (8–16% reduction). However, 10 μM BUM resulted in a similar

block of shoot PAT (76% reduction) compared with NPA (not shown). This demonstrates the ability of BUM to act as a PAT inhibitor but suggests different affinities to transporters or an altered presence of targets in the root and shoot.

Second, we employed an IAA-specific microelectrode that has become a reliable tool for non-invasively recording IAA influxes into the root transition zone (11, 12, 34, 35). IAA influx in this zone is characterized by a distinct peak at 200 μm from the root tip and is consistent with the current auxin reflux model (8) and a measure for PAT. In agreement with DR5-GFP imaging and PAT measurements, IAA influx peaks were strongly and similarly reduced by 5 μM BUM or NPA (Fig. 5*B*). The magnitude of inhibition caused by BUM and NPA phenocopies genetic reductions of influx peaks found for single *ABCB1 or ABCB19* auxin transporter loss-of-function roots (11). However, gravacin, a recently identified inhibitor of gravitropism (23), had a less pronounced inhibitory effect on IAA influx as with *abcb1* or *abcb19* single mutant roots (11). This is in good agreement with the reported concept that gravacin binds to and inhibits primarily ABCB19 and not ABCB1 (23). Interestingly, BUM resulted in an additional shift of the influx

maximum ~40 nm in the apical direction (not found with NPA or gravacin) that might account for more drastic growth inhibition despite similar reduction of influx peaks. Differences in the magnitude of inhibition of root PAT caused by NPA and BUM measured by means of droplet application (Fig. 5*A*) or an IAA-selective electrode (Fig. 5*B*) might have systematic reasons caused by different inhibitor concentration and application duration and site (either applied to the (root) tip or in the electrode bath).

ABCBs Are the Primary Targets of BUM and NPA—The current picture is that ABCBs and the interacting ABCB1,19-regulator, TWD1/FKBP42, but probably not PIN proteins represent predicted low and high affinity, respectively, NPA-binding proteins (11). This is supported by recent studies demonstrating ABCB1 and ABCB19 to bind NPA resulting in inhibition of efflux activity (5, 11, 23), whereas PIN1 did not seem to bind NPA (23).

Our data so far suggested that auxin exporters, the primary control units of PAT, might be the direct targets of BUM action. Our data showing that lateral root formation in *abcb1* but not in *pin2* roots is BUM-insensitive (Fig. 2*C*) point to the subclass of ABCBs as possible BUM targets. In order to clarify which subclass of auxin exporters is a direct target of BUM, we quantified IAA export activities of the most prominent members of the ABCB and PIN subclass, ABCB1,19 and PIN1,2, by heterologous expression in yeast. IAA export analysis in bakers' yeast clearly demonstrated that ABCB1 but not PIN2 is inhibited significantly by BUM and by NPA although to a lesser extent (supplemental Fig. S6). Inhibition was specific because background (vector control) inhibition by NPA/BUM was negligible (3.3/6.3%). Moreover, background activities monitored simultaneously by the non-ABCB1 substrate benzoic acid were not significantly affected (supplemental Fig. S6). Because *Saccharomyces cerevisiae* does not allow expression of functional PIN1 and ABCB19/MDR1/PGP19, both known to provide basipetal shoot (20) and acropetal root transport (51), most probably due to hyperglycosylation and unfavorable membrane compositions (5, 9), we expressed them in the fission yeast. *S. pombe* has recently been reported as the system of choice for plant auxin transporters, most likely because it offers polarized, sterol-enriched plasma-membrane microdomains and reduced glycosylation (36, 52). As described previously (36), ABCB1,19 and PIN1,2 were able to efficiently export IAA, resulting in 50–60% of vector control loading (Fig. 5*C*). As found with bakers' yeast, BUM and NPA inhibited IAA export (increase to vector control loading of roughly 40–50%) for ABCB1,19, whereas the increase in IAA loading for PIN1,2 was in the range found for the vector control (increase of 8–10%). This indicates that ABCBs, unlike PINs, are BUM/NPA targets, whereas again BUM at the same concentrations (10 μM) used was more efficient in ABCB inhibition than NPA.

NPA binding studies using *Arabidopsis* microsomes support the yeast transport data by demonstrating that ABCB1 and ABCB19 but again not PIN2 (87.0 ± 13.5% of wild type) function as NPA-binding proteins (Fig. 6*A*).[6] Interestingly, ABCB19

---

[6] Note that due to the sterility of homozygous *pin1* it is not possible to gain enough material to perform binding assays for *pin1*.
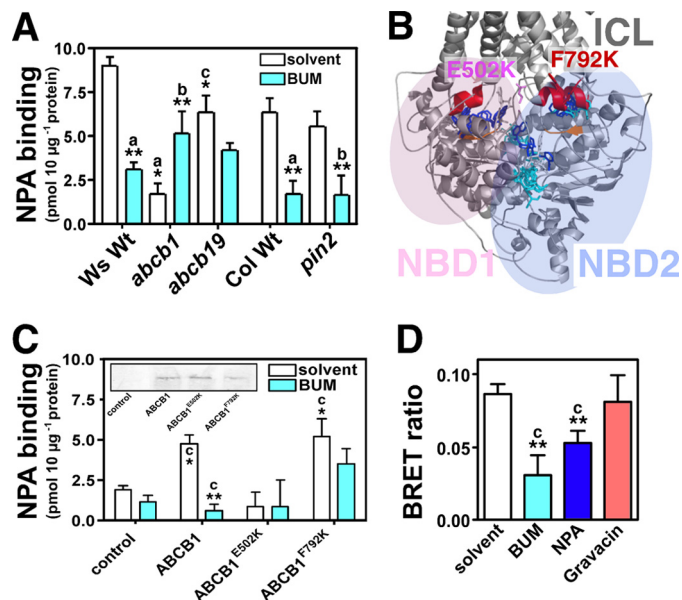

FIGURE 6. **BUM competes for NPA binding to ABCB-type auxin exporters.** *A*, BUM competes for NPA binding to wild type and *pin2* microsomes but to a lesser extent to *abcb* membranes (mean ± S.E. (*error bars*); n = 4). *B*, *in silico* drug binding to the N- and C-terminal ABCB1 nucleotide binding folds (NBD1 and -2) suggest overlapping and distinct inhibitor binding pockets for BUM (*cyan*) and NPA (*blue*). Note that NPA docks to pockets flanked by coupling helices (*red*) and Q loop (*orange*) of NBD1 and NBD2, whereas BUM docks only to the pocket corresponding to NBD2. Relevant residues Glu[502] and Phe[792] mutagenized under *C* are represented as *pink* and *red sticks*. *C*, site-directed mutagenesis of functional key residues predicted under *B* abolishes NPA/BUM binding (E502K) or reduces BUM competition (F792K); mean ± S.E. (n = 4). ABCB1 expression validated by Western analysis using anti-ABCB1/19 (5) is not significantly altered (*inset*). *D*, BUM, like NPA (each 5 μM), disrupts TWD1-ABCB1 interaction monitored by yeast BRET assays, whereas gravacin had only minor effects (mean ± S.E.; n = 4). Significant differences (analysis of variance using Tukey's test for multiple comparisons: $p < 0.001$ (*a*); $p < 0.01$ (*b*); $p < 0.05$ (*c*)) from wild type (*A*) or vector controls (*C*) or between inhibitor and solvent treatments are indicated by *one* or *two asterisks*, respectively.

(70.4 ± 10.8% of wild type) contributes less to NPA binding compared with ABCB1 (19.1 ± 6.5%), which is in contrast to previous data that determined ABCB19 as the primary NBP (23). However, the previous study employed different starting material and microsomal preparations for the binding studies that might influence individual ABCB abundance (23). Importantly, BUM competes drastically for NPA binding on both wild type ecotypes (65–73% reduction) and *pin2* microsomes (70%) but not on *abcb1* and only to a minor, non-significant degree on *abcb19* membranes. NPA binding and BUM competition is specific because binding of the nonspecific control, BA, assayed in parallel was a factor 10 lower, whereas BUM competition was strongly reduced on wild-type (25–58% reduction) and *pin2* (34% reduction) membranes (supplemental Fig. S7). Enhanced NPA binding caused by BUM competition on *abcb1* membranes might be indirect because the same tendency was found with BA. In line with this, our previous work has demonstrated that single loss of *abcb* or *pin* functionality reduces the transport specificity and NPA sensitivity of the ABCB-PIN export complex (9).

In order to mechanistically understand functional differences between BUM and NPA inhibitor activities, we computed BUM and NPA docking to the *Arabidopsis* ABCB1 structure that was modeled on the crystal structure of ABCB-related multidrug efflux pump Sav1866 (53). In the *in silico* analyses,

both inhibitors dock predominantly to both nucleotide binding domains (NBDs), whereas only minor apparent binding was found with the transmembrane domains (TMDs; not shown). NPA was predicted to bind interestingly primarily to grooves between coupling helices and Q loops (Fig. 6B), the main ABCB mechanics connecting NBDs and TMDs. In contrast, BUM was only predicted to dock to the corresponding pocket of NBD2 and additionally to an NBD1-NBD2 interface. Interestingly, BUM additionally has an apparent high affinity (around −50 kcal/mol) to a second NBD1-NBD2 interface where no NPA binding was predicted; this might account for its severe inhibition.

In order to experimentally validate our assumptions from *in silico* structure modeling and drug binding, we chose to neutralize key residues Glu^{502} and Phe^{792} situated in the ABCB1 cross-loop and coupling helix of NBD2 (53) by site-directed mutagenesis and measure subsequent NPA binding. Not unexpectedly, the E502K mutation abolished NPA binding and thus also BUM competition because mutations in the cross-loop have been suggested to alter drastically ABCB architecture (53). More interestingly, F792K mutagenesis in the C-terminal coupling helix did not affect NPA binding but significantly reduced BUM competition. This suggests that a single point mutation is able to exclude selectively BUM (but not NPA) from a putative BUM/NPA binding pocket (Fig. 6B). Although one should keep in mind that the drastic mutagenesis in essential mechanical key units of ABCB1, such as the cross-loop and the coupling helix, might as such affect fundamentally the functional interaction of NBDs and TMDs, our data provide a mechanistically explanation for overlapping and distinct effects of BUM/NPA on plant physiology development.

NPA was recently demonstrated to block ABCB-mediated auxin export by disrupting TWD1-ABCB1 interaction (5, 11). Not surprisingly, BUM also disrupted TWD1-ABCB1 interaction as monitored by established yeast BRET assays (11) (Fig. 6D). The fact that, based on docking studies, BUM probably binds, like NPA, to the ABCB1 NBD2 is in line with experimental data (5, 11, 12) and recent modeling of TWD1-ABC interfaces (54). More severe disruption, probably caused by BUM binding to NBD1-NBD2 interfaces, suggests that BUM achieves TWD1-ABCB1 disruption either by long range, intramolecular movements proposed for ABCBs (53, 55) or by binding to TWD1 in analogy to NPA (11). Although *twd1* is gravacin-insensitive (23), gravacin does not disrupt TWD1-ABCB1 interaction. Therefore, TWD1 is apparently not a direct target of gravacin as has been proposed recently (23).

DISCUSSION

Recent analyses of PIN and ABCB transport mechanisms suggest independent (or sometimes even opposite) and at certain domains additive and synergistic actions (9, 10). In this study, we have identified by means of chemical genomics a novel ATI that efficiently blocks auxin-related plant physiology and development. Quantification of physiological parameters, drug binding, and transport data indicates that ABCBs, primarily ABCB1, are direct BUM/NPA targets, whereas PINs are apparently less affected, which is in agreement with previous findings on NPA (14, 22, 23). This makes BUM a valuable tool for auxin research, allowing differentiation between ABCB-

and PIN-mediated efflux systems. On the other hand, our work also suggests that pin-formed inflorescences, which are caused by BUM and NPA and that phenocopy *PIN1* loss-of-function mutations are primarily caused by ABCB transport inhibition of the functional ABCB-PIN efflux complex.

Our findings also demonstrate that BUM inhibition, like NPA inhibition, is light-dependent. This leads to the suggestion that ABCBs, obviously the cellular targets of BUM- and NPA-induced inhibition in *Arabidopsis*, are part of a light-controlled developmental pathway, which is in agreement with the concept that auxin has a more important role in elongation and bending responses in the light (44, 45). This concept was recently genetically supported by demonstrating that the photoreceptors, phytochromes and cryptochromes, regulate differential growth of *Arabidopsis* hypocotyls in an ABCB-dependent manner (45).

In many physiological respects and partially also structurally, BUM resembles NPA functionality. Based on our transport and drug binding data, both have a stronger effect on ABCB1 than on ABCB19 (Figs. 5 and 6). However, BUM has the advantage of not showing activation of plant growth at lower concentrations and acting roughly a factor of 30 stronger than NPA, which seems to be mainly caused by apically shifted root influx maxima. This again might be the result of altered binding preferences or affinities to the ABCBs. An alternative, simpler explanation that we cannot rule out at the moment is that BUM, being less hydrophobic compared with NPA, has a higher solubility. BUM shares this higher apparent solubility with the phytotropin l-(2′-carboxyphenyl)-3-phenylpropane-1,3-dione, which competes for the same binding site and does affect the same processes of auxin transport and geotropic curvature as NPA (56). However, based on our binding, the primary BUM target seems to be ABCB1. This makes BUM complementary to NPA that has been shown to affect besides ABCB19 also other ABCBs (5, 22, 57). Most interestingly, BUM reveals a more drastic effect (even at lower concentrations) on root transport (Fig. 5) and root elongation (Fig. 2) than found in the hypocotyl in comparison with NPA, which shows an inverse behavior. The molecular reasons are unknown and under current investigation. However, this finding is in agreement with higher ABCB19 expression in the hypocotyl (9) and a lower inhibition ABCB19 by BUM compared with ABCB1.

BUM apparently also acts differently compared with the recently identified ATI, gravacin, which primarily inhibits ABCB19 (23). However, as shown by BRET analysis, BUM, unlike gravacin, also alters TWD1 function, suggesting that BUM might indirectly also regulate ABCB19 activity by disrupting TWD1-ABCB19 interaction. Another advantage is that BUM, unlike gravacin, apparently does not interfere with ABCB trafficking.

Besides its academic usage as an ATI and its obvious potential as powerful weed herbicide, BUM might have a direct clinical impact because multidrug resistance toward many anticancer drugs is largely caused by human ABCB1, leading often to chemotherapy ineffectiveness. Interestingly, human and plant ABCBs share broad inhibitor sensitivities, which was demonstrated for the flavonol quercetin, which acts both as modulator of auxin transport and as inhibitor of mammalian

and plant ABCBs, and for clinically relevant ABCB inhibitors, like cyclosporine A and verapamil (5, 12). Based on our findings, plant ABCB inhibitors, such as BUM and NPA, are therefore *bona fide* human ABCB inhibitors that might suppress multi-drug resistance when co-administered with anti-cancer drugs.

REFERENCES

1. Blakeslee, J. J., Peer, W. A., and Murphy, A. S. (2005) *Curr. Opin. Plant Biol.* **8,** 494–500
2. Kepinski, S., and Leyser, O. (2005) *Curr. Biol.* **15,** R208–R210
3. Vieten, A., Sauer, M., Brewer, P. B., and Friml, J. (2007) *Trends Plant Sci.* **12,** 160–168
4. Benjamins, R., and Scheres, B. (2008) *Annu. Rev. Plant Biol.* **59,** 443–465
5. Geisler, M., Blakeslee, J. J., Bouchard, R., Lee, O. R., Vincenzetti, V., Bandyopadhyay, A., Titapiwatanakun, B., Peer, W. A., Bailly, A., Richards, E. L., Ejendal, K. F., Smith, A. P., Baroux, C., Grossniklaus, U., Müller, A., Hrycyna, C. A., Dudler, R., Murphy, A. S., and Martinoia, E. (2005) *Plant J.* **44,** 179–194
6. Geisler, M., and Murphy, A. S. (2006) *FEBS Lett.* **580,** 1094–1102
7. Petrásek, J., Mravec, J., Bouchard, R., Blakeslee, J. J., Abas, M., Seifertová, D., Wisniewska, J., Tadele, Z., Kubes, M., Covanová, M., Dhonukshe, P., Skupa, P., Benková, E., Perry, L., Krecek, P., Lee, O. R., Fink, G. R., Geisler, M., Murphy, A. S., Luschnig, C., Zazímalová, E., and Friml, J. (2006) *Science* **312,** 914–918
8. Blilou, I., Xu, J., Wildwater, M., Willemsen, V., Paponov, I., Friml, J., Heidstra, R., Aida, M., Palme, K., and Scheres, B. (2005) *Nature* **433,** 39–44
9. Blakeslee, J. J., Bandyopadhyay, A., Lee, O. R., Mravec, J., Titapiwatanakun, B., Sauer, M., Makam, S. N., Cheng, Y., Bouchard, R., Adamec, J., Geisler, M., Nagashima, A., Sakai, T., Martinoia, E., Friml, J., Peer, W. A., and Murphy, A. S. (2007) *Plant Cell* **19,** 131–147
10. Mravec, J., Kubes, M., Bielach, A., Gaykova, V., Petrásek, J., Skŭpa, P., Chand, S., Benková, E., Zazímalová, E., and Friml, J. (2008) *Development* **135,** 3345–3354
11. Bailly, A., Sovero, V., Vincenzetti, V., Santelia, D., Bartnik, D., Koenig, B. W., Mancuso, S., Martinoia, E., and Geisler, M. (2008) *J. Biol. Chem.* **283,** 21817–21826
12. Bouchard, R., Bailly, A., Blakeslee, J. J., Oehring, S. C., Vincenzetti, V., Lee, O. R., Paponov, I., Palme, K., Mancuso, S., Murphy, A. S., Schulz, B., and Geisler, M. (2006) *J. Biol. Chem.* **281,** 30603–30612
13. Cox, D. N., and Muday, G. K. (1994) *Plant Cell* **6,** 1941–1953
14. Luschnig, C. (2001) *Curr. Biol.* **11,** R831–R833
15. Michalke, W., Katekar, G. F., and Geissler, A. E. (1992) *Planta* **187,** 254–260
16. Petrásek, J., Cerná, A., Schwarzerová, K., Elckner, M., Morris, D. A., and Zazímalová, E. (2003) *Plant Physiol.* **131,** 254–263
17. Sussman, M. R., and Gardner, G. (1980) *Plant Physiol.* **66,** 1074–1078
18. Bernasconi, P., Patel, B. C., Reagan, J. D., and Subramanian, M. V. (1996) *Plant Physiol.* **111,** 427–432
19. Lomax, T. L., Muday, G. K., and Rubery, P. H. (1995) in *Plant Hormones: Physiology, Biochemistry, and Molecular Biology* (Davies, P. J., ed) pp. 509–530, Kluwer, Dordrecht, The Netherlands
20. Okada, K., Ueda, J., Komaki, M. K., Bell, C. J., and Shimura, Y. (1991) *Plant Cell* **3,** 677–684
21. Geldner, N., Friml, J., Stierhof, Y. D., Jürgens, G., and Palme, K. (2001) *Nature* **413,** 425–428
22. Nagashima, A., Uehara, Y., and Sakai, T. (2008) *Plant Cell Physiol.* **49,** 1250–1255
23. Rojas-Pierce, M., Titapiwatanakun, B., Sohn, E. J., Fang, F., Larive, C. K., Blakeslee, J., Cheng, Y., Cutler, S. R., Peer, W. A., Murphy, A. S., and Raikhel, N. V. (2007) *Chem. Biol.* **14,** 1366–1376
24. Murphy, A. S., Hoogner, K. R., Peer, W. A., and Taiz, L. (2002) *Plant Physiol.* **128,** 935–950
25. Noh, B., Murphy, A. S., and Spalding, E. P. (2001) *Plant Cell* **13,** 2441–2454
26. Armstrong, J. I., Yuan, S., Dale, J. M., Tanner, V. N., and Theologis, A. (2004) *Proc. Natl. Acad. Sci. U.S.A.* **101,** 14978–14983
27. Zhao, Y., Dai, X., Blackwell, H. E., Schreiber, S. L., and Chory, J. (2003) *Science* **301,** 1107–1110
28. Norambuena, L., Hicks, G. R., and Raikhel, N. V. (2009) *Methods in Molecular Biology* **495,** 133–143
29. Robert, S., Chary, S. N., Drakakaki, G., Li, S., Yang, Z., Raikhel, N. V., and Hicks, G. R. (2008) *Proc. Natl. Acad. Sci. U.S.A.* **105,** 8464–8469
30. Surpin, M., Rojas-Pierce, M., Carter, C., Hicks, G. R., Vasquez, J., and Raikhel, N. V. (2005) *Proc. Natl. Acad. Sci. U.S.A.* **102,** 4902–4907
31. Savaldi-Goldstein, S., Baiga, T. J., Pojer, F., Dabi, T., Butterfield, C., Parry, G., Santner, A., Dharmasiri, N., Tao, Y., Estelle, M., Noel, J. P., and Chory, J. (2008) *Proc. Natl. Acad. Sci. U.S.A.* **105,** 15190–15195
32. Luschnig, C., Gaxiola, R. A., Grisafi, P., and Fink, G. R. (1998) *Genes Dev.* **12,** 2175–2187
33. Lewis, D. R., and Muday, G. K. (2009) *Nat. Protoc.* **4,** 437–451
34. Mancuso, S., Marras, A. M., Magnus, V., and Baluska, F. (2005) *Anal. Biochem.* **341,** 344–351
35. Santelia, D., Vincenzetti, V., Azzarello, E., Bovet, L., Fukao, Y., Düchtig, P., Mancuso, S., Martinoia, E., and Geisler, M. (2005) *FEBS Lett.* **579,** 5399–5406
36. Yang, H., and Murphy, A. S. (2009) *Plant J.* **59,** 179–191
37. Morris, D. A. (2000) *Plant Growth Regul.* **32,** 161–172
38. Santelia, D., Henrichs, S., Vincenzetti, V., Sauer, M., Bigler, L., Klein, M., Bailly, A., Lee, Y., Friml, J., Geisler, M., and Martinoia, E. (2008) *J. Biol. Chem.* **283,** 31218–31226
39. Benková, E., Michniewicz, M., Sauer, M., Teichmann, T., Seifertová, D., Jürgens, G., and Friml, J. (2003) *Cell* **115,** 591–602
40. Bhalerao, R. P., Eklöf, J., Ljung, K., Marchant, A., Bennett, M., and Sandberg, G. (2002) *Plant J.* **29,** 325–332
41. Casimiro, I., Beeckman, T., Graham, N., Bhalerao, R., Zhang, H., Casero, P., Sandberg, G., and Bennett, M. J. (2003) *Trends Plant Sci.* **8,** 165–171
42. Rashotte, A. M., DeLong, A., and Muday, G. K. (2001) *Plant Cell* **13,** 1683–1697
43. Achard, P., Vriezen, W. H., Van Der Straeten, D., and Harberd, N. P. (2003) *Plant Cell* **15,** 2816–2825
44. Jensen, P. J., Hangarter, R. P., and Estelle, M. (1998) *Plant Physiol.* **116,** 455–462
45. Nagashima, A., Suzuki, G., Uehara, Y., Saji, K., Furukawa, T., Koshiba, T., Sekimoto, M., Fujioka, S., Kuroha, T., Kojima, M., Sakakibara, H., Fujisawa, N., Okada, K., and Sakai, T. (2008) *Plant J.* **53,** 516–529
46. Rashotte, A. M., Brady, S. R., Reed, R. C., Ante, S. J., and Muday, G. K. (2000) *Plant Physiol.* **122,** 481–490
47. Swarup, R., Kramer, E. M., Perry, P., Knox, K., Leyser, H. M., Haseloff, J., Beemster, G. T., Bhalerao, R., and Bennett, M. J. (2005) *Nat. Cell Biol.* **7,** 1057–1065
48. Ottenschläger, I., Wolff, P., Wolverton, C., Bhalerao, R. P., Sandberg, G., Ishikawa, H., Evans, M., and Palme, K. (2003) *Proc. Natl. Acad. Sci. U.S.A.* **100,** 2987–2991
49. Peer, W. A., Bandyopadhyay, A., Blakeslee, J. J., Makam, S. N., Chen, R. J., Masson, P. H., and Murphy, A. S. (2004) *Plant Cell* **16,** 1898–1911
50. Vieten, A., Vanneste, S., Wisniewska, J., Benková, E., Benjamins, R., Beeckman, T., Luschnig, C., and Friml, J. (2005) *Development* **132,** 4521–4531
51. Wu, G., Lewis, D. R., and Spalding, E. P. (2007) *Plant Cell* **19,** 1826–1837
52. Titapiwatanakun, B., Blakeslee, J. J., Bandyopadhyay, A., Yang, H., Mravec, J., Sauer, M., Cheng, Y., Adamec, J., Nagashima, A., Geisler, M., Sakai, T., Friml, J., Peer, W. A., and Murphy, A. S. (2009) *Plant J.* **57,** 27–44
53. Dawson, R. J., and Locher, K. P. (2006) *Nature* **443,** 180–185
54. Granzin, J., Eckhoff, A., and Weiergräber, O. H. (2006) *J. Mol. Biol.* **364,** 799–809
55. Locher, K. P. (2009) *Philos. Trans. R. Soc. Lond. B. Biol. Sci.* **364,** 239–245
56. Katekar, G. F., and Geissler, A. E. (1980) *Plant Physiol.* **66,** 1190–1195
57. Terasaka, K., Blakeslee, J. J., Titapiwatanakun, B., Peer, W. A., Bandyopadhyay, A., Makam, S. N., Lee, O. R., Richards, E. L., Murphy, A. S., Sato, F., and Yazaki, K. (2005) *Plant Cell* **17,** 2922–2939